

# Accounting for the effect of horizontal gradients in limb measurements of scattered sunlight

**J. Puķīte<sup>1,2</sup>, S. Kühl<sup>1</sup>, T. Deutschmann<sup>3</sup>, U. Platt<sup>3</sup>, and T. Wagner<sup>1</sup>**

<sup>1</sup>Max Planck Institute for Chemistry, J.J. Becher Weg 27, 55128 Mainz, Germany

<sup>2</sup>Institute of Atomic Physics and Spectroscopy, University of Latvia, Raina Bulv. 19, Riga, 1586, Latvia

<sup>3</sup>Institute of Environmental Physics, University of Heidelberg, Im Neuenheimer Feld 229, 69120 Heidelberg, Germany

Received: 12 October 2007 – Accepted: 7 November 2007 – Published: 19 November 2007

Correspondence to: J. Puķīte (janis.pukite@mpch-mainz.mpg.de)

**Horizontal gradients  
in limb  
measurements of  
scattered sunlight**

J. Puķīte et al.

Title Page

Abstract

Introduction

Conclusions

References

Tables

Figures

⏪

⏩

◀

▶

Back

Close

Full Screen / Esc

Printer-friendly Version

Interactive Discussion

## Abstract

Limb measurements provided by the SCanning Imaging Absorption spectrometer for Atmospheric CHartographyY (SCIAMACHY) on the ENVISAT satellite allow retrieving stratospheric profiles of various trace gases on a global scale, among them BrO for the first time. For limb observations in the UV/VIS spectral region the instrument measures scattered light with a complex distribution of light paths: the light is measured at different elevation angles and can be scattered or absorbed in the atmosphere or reflected by the ground. By means of spectroscopy and radiative transfer modelling the measurements can be inverted to retrieve the vertical distribution of stratospheric trace gases.

A full spherical 3-D Monte Carlo radiative transfer model “Tracy-II” is applied in this study. The Monte Carlo method benefits from conceptual simplicity and allows realizing the concept of full spherical geometry of the atmosphere and also its 3-D properties, which is important for a realistic description of the limb geometry. Furthermore it allows accounting for horizontal gradients in the distribution of trace gases.

In this study the effect of horizontal inhomogeneous distributions of trace gases on the retrieval of profiles from limb measurements of scattered UV/VIS light is investigated. We introduce a method to correct for this effect by combining consecutive limb scanning sequences and utilizing the overlap in their measurement sensitivity regions. It is found that if horizontal inhomogeneity is not properly accounted for, typical errors of 20% for NO<sub>2</sub> and up to 50% for OCIO around the altitude of the profile peak can arise for measurements close to the Arctic polar vortex boundary in boreal winter.

## 1 Introduction

Compared to nadir observations (i.e. space borne instruments is looking perpendicularly to the surface of the Earth) which provide knowledge of the total column density and very limited information about profile, measurements in limb geometry (i.e. tan-

ACPD

7, 16155–16183, 2007

### Horizontal gradients in limb measurements of scattered sunlight

J. Puķīte et al.

Title Page

Abstract

Introduction

Conclusions

References

Tables

Figures

⏪

⏩

◀

▶

Back

Close

Full Screen / Esc

Printer-friendly Version

Interactive Discussion

gential view in respect to the Earth surface) provide further opportunities to extract height resolved profile information. This is achieved by measuring backscattered light from air masses at different elevation angles corresponding to different tangent heights. Satellite instruments such as the Optical Spectrograph and Infrared Imager System (OSIRIS) on the Odin satellite (Llewellyn et al., 2004), SCIAMACHY on ENVISAT (Bovensmann et al., 1999), and also the Stratospheric Aerosol and Gas Experiment (SAGE III) on the Meteor 3 have limb observation possibilities (Rault, 2005) in the UV/VIS spectral region.

The SCIAMACHY instrument on the ENVISAT satellite whose measurements are applied in this study is operating in a near polar sun synchronous orbit with an inclination from the equatorial plane of  $\sim 98.5^\circ$ . It is performing one orbit in approximately 100 min with equator crossing time of 10:00 in descending mode. The satellite probes the atmosphere at the day side of Earth in alternating sequences of nadir and limb measurements. Limb scans in one scanning sequence are performed with approximately 3.3 km elevation steps at the tangent point (TP). The swath across flying direction is 960 km at the TP and consists of 4 pixels. The field of view (FOV) is  $0.045^\circ$  in elevation and  $1.8^\circ$  in azimuth. This corresponds to approximately 2.5 km and 110 km at TP, respectively. SCIAMACHY is measuring in the UV-VIS-NIR spectral range from 240 to 2380 nm with a spectral resolution of approximately 0.25 to 0.55 nm in the UV-VIS range. More instrumental details can be found in Bovensmann et al. (1999).

The limb geometry is characterized by very slant and thus long lines of sight (LOS) through the atmosphere crossing extended volumes of air masses. In existing limb retrieval algorithms from SCIAMACHY limb spectra (Sioris et al., 2004; Rozanov et al., 2005; Köhl, 2005; Sinnhuber et al., 2005; Sioris et al., 2006; Puķīte et al., 2006; Köhl et al., 2007) the retrieval of profiles is performed for every limb scanning sequence separately.

However, large variability in the concentrations of the photochemically active trace gases can occur along the long line of sight: If the model assumes horizontally homogeneous distribution, horizontal inhomogeneity in the spatial distributions of atmospheric

---

## Horizontal gradients in limb measurements of scattered sunlight

J. Puķīte et al.

---

Title Page

Abstract

Introduction

Conclusions

References

Tables

Figures

◀

▶

◀

▶

Back

Close

Full Screen / Esc

Printer-friendly Version

Interactive Discussion

trace gases is introducing systematical errors in profile retrievals from limb measurements. Approaches to correct for this effect applying photochemical modelling have been described recently (Natarajan et al., 2005; McLinden et al., 2006; Sioris et al., 2006).

5 The aim of this study is to demonstrate a possibility to correct for the horizontal gradient effect from the observations by combining consecutive limb scanning sequences without input from chemical modelling. For infrared spectra, a direct inversion algorithm developed for MIPAS instrument (also flown on ENVISAT) was introduced to retrieve temperature, pressure and trace gases simultaneously for all limb scanning sequences  
10 of one orbit taking into account horizontal variability (Carlotti et al., 2001; Ridolfi et al., 2004; Carlotti et al., 2006).

In this study a distance of only  $3.75^\circ$  between satellite positions (corresponding to approx. 415 km along the Earth's surface) of consecutive scanning states for the northern part of a SCIAMACHY orbit will be used to study the impact of horizontal in-  
15 homogeneity for limb measurements of scattered light in the UV/VIS spectral range. For that purpose, an overlap between largely extended sensitivity regions of consecutive scanning sequences is utilized. For our retrieval we apply a two step method (Kühl, 2005; Puķīte et al., 2006; Kühl et al., 2007). Similar approaches have been described by Haley et al. (2004), Krecl et al. (2006), Sioris et al. (2006).

20 The 3-D full spherical Monte Carlo radiative transfer modelling (RTM) allows the introduction of a 2-D air mass factor concept, varying not only in altitude but also in latitude (for definition please refer to Sect. 4.2). It enables the estimation of sensitivity regions of limb measurements and allows the simultaneous inversion of many limb scanning sequences, thereby providing the 2-D field of spatial distribution of concentrations of trace gases. In this article we investigate how the 2-D air mass factor concept  
25 can be applied to correct for the horizontal gradient effect. The retrieved profiles resulting by applying either 1-D or 2-D air mass factors are compared for selected case studies.

---

## Horizontal gradients in limb measurements of scattered sunlight

J. Puķīte et al.

---

Title Page

Abstract

Introduction

Conclusions

References

Tables

Figures

⏪

⏩

◀

▶

Back

Close

Full Screen / Esc

Printer-friendly Version

Interactive Discussion

## 2 Retrieval algorithm

An algorithm for the retrieval of NO<sub>2</sub>, BrO and OCIO vertical profiles from the SCIAMACHY limb measurements was developed in our group (Kühl, 2005; Puķīte et al., 2006). It allows the efficient retrieval of trace gas profiles, and shows a good agreement of the retrieved BrO and NO<sub>2</sub> profiles with balloon measurements (Dorf et al., 2006; Butz et al., 2006; Kühl et al., 2007). The retrieval of vertical trace gas profiles from SCIAMACHY measured limb spectra is done in two steps as illustrated in Fig. 1. In the first step, slant column densities (SCDs) of the trace gases are derived from the SCIAMACHY limb spectra by Differential Optical Absorption Spectroscopy (DOAS). Second, the trace gas SCDs are converted into vertical concentration profiles applying RTM. Inversion is performed either by the optimal estimation method or a least squares approach. For the algorithm details please refer to Puķīte et al. (2006).

## 3 Radiative transfer modelling

We apply the 3-D full spherical Monte Carlo radiative transfer model “Tracy-II” (Deutschmann and Wagner, 2007; Wagner et al., 2007) to calculate box AMFs (i.e. the ratio between slant and vertical column for the considered atmospheric region) which are necessary to retrieve number density profiles of trace gases from the measured SCDs. The largest advantage of Monte Carlo models in limb geometry is that they properly take into account Earth’s sphericity both for single and multiple scattering (Oikarinen et al., 1999; Loughman et al., 2004). Furthermore they also provide the possibility to simulate to a high degree an inhomogeneous atmosphere. The model does not take into account refraction since it would require additional computer power but its effect was found to be negligible for altitudes above 12 km (see e.g. Sioris et al., 2006). Also aerosols and clouds are not included. The aerosol extinction is much lower compared to extinction by Rayleigh scattering in the stratosphere. Also, because of the slantness of limb observations the measurements are practically insensitive to

### Horizontal gradients in limb measurements of scattered sunlight

J. Puķīte et al.

Title Page

Abstract

Introduction

Conclusions

References

Tables

Figures

⏪

⏩

◀

▶

Back

Close

Full Screen / Esc

Printer-friendly Version

Interactive Discussion

the atmosphere below the tangent height.

For temperature, pressure and ozone we apply a model simulation provided by Brühl and Crutzen (1993). It should be noted that in some individual cases temperature, pressure and ozone concentration might differ considerably. From sensitivity studies we found that the related errors in profile retrieval can be up to 10%. However the conclusions of this study are not affected by these systematic effects.

### 3.1 Spatial sensitivity

The instrument measures light scattered into the LOS either directly from the incoming solar radiation, or being scattered previously by the atmosphere or the ground below. The limb geometry is characterized by relatively long paths of light along the LOS after the last scattering event in comparison to the paths before the atmospheric last scattering event. Along the LOS the instrument has different sensitivities for different locations in the atmosphere. In general the instrument exhibits higher sensitivity to air masses closer to instrument since the light contributing to the measurement integrates along the line of sight (see schematic view in Fig. 2). The sensitivity varies considerably for the different elevations, mainly due to scattering on air molecules. Also absorption (especially ozone) and scattering by aerosols, clouds and reflection at the ground modify the measured light intensity. For high altitudes, where the atmosphere is optically transparent, a nearly symmetrical distribution across the tangent point (TP) of photons being scattered into the LOS is observed by the model. For the retrieval at low altitudes a limiting factor is the large possibility for Rayleigh scattering i.e. the atmosphere is optically thick. Furthermore, usually clouds are present along the LOS at low altitudes, also preventing sensitivity for low atmospheric layers.

Therefore at low elevations with an optically dense atmosphere, more photons contribute from volumes of the side between TP and instrument. Thus, besides the low sensitivity for altitudes below 12–15 km a shift of the sensitivity towards regions on the side between TP and instrument occurs. This also means (as it will be seen later in Sect. 4.2) that the measured spectra practically contain no information about regions

## Horizontal gradients in limb measurements of scattered sunlight

J. Puķīte et al.

Title Page

Abstract

Introduction

Conclusions

References

Tables

Figures

⏪

⏩

◀

▶

Back

Close

Full Screen / Esc

Printer-friendly Version

Interactive Discussion

around the TP for low elevations.

### 3.2 Horizontal gradients

Photochemically active species like BrO, NO<sub>2</sub> and OCIO can vary significantly in space and time due to their dependence on solar illumination, atmospheric chemistry and transport. The large extension over which satellite limb observations are sensitive requires the consideration of gradients in the trace gas distributions. Since the instrument is more sensitive to the air masses closer to it, this side will have a larger effect on measurement results. If horizontal gradients exist, algorithms which do not account for the horizontal variation of trace gases will introduce errors in the retrieval: If the concentration gradient in the instrument direction is positive this will lead to a higher concentration as in reality and the peak values will tend to appear at lower altitudes: Higher concentration values towards the instrument will be wrongly accounted for the place where the measurement is assumed to be taken (for the TP). Vice versa for negative gradients the opposite is the case.

Algorithms assuming homogeneous horizontal distributions do not take into account that the LOS is crossing regions with concentrations different to those that appear around tangent point. For situations with significant horizontal inhomogeneous distribution this will lead to increased systematic errors in the profile retrieval.

## 4 Two-dimensional retrieval

### 4.1 The retrieval approach

In order to account for possible gradients in the profile retrieval we suggest a two dimensional retrieval where we combine consecutive limb scanning sequences and describe the measurement as a superposition not only regarding varying altitude but also latitude parameters. In this approach we invert measurement sequences of one orbit

## Horizontal gradients in limb measurements of scattered sunlight

J. Puķīte et al.

Title Page

Abstract

Introduction

Conclusions

References

Tables

Figures

⏪

⏩

◀

▶

Back

Close

Full Screen / Esc

Printer-friendly Version

Interactive Discussion

simultaneously, including in the retrieval the information about the horizontal sensitivity of the measurements. Thus, the 2-D approach is distinguishing between air volumes at different regions along line of sight. Precondition for an improvement with respect to the one-dimensional algorithm is that the change of the atmospheric trace gas concentrations (particularly because of SZA change and transport of air) in time is negligible. The SZA change in time (in January) for consecutive scanning sequence in the North is from  $\sim 0.025^\circ$  (most northern state) to  $\sim 0.07^\circ$  (around  $60^\circ$  N) during the time ( $\sim 1$  min) which is necessary to cross the distance between two following scanning sequences (Fig. 3, left panel indicated with red circle). This difference in the SZA is not resulting in significant profile changes of the considered absorbers. Also the spatial distance between the following scanning sequences should be small enough so that they in some extent overlap (see Fig. 3) and at least be less than the sensitivity region of one limb measurement. Both criteria are fulfilled for the northern part of SCIAMACHY orbits, where the first 3 or 4 limb scanning sequences (indicated for an example in the right panel of Fig. 3) are performed without nadir observations in between.

#### 4.2 Two-dimensional box air mass factors

Figure 4 shows 1-D box AMFs calculated by the RTM Tracy-II as function of tangent height. For an instrument elevation  $z$  they are defined as ratio of the slant column density  $SCD_{iz}$  of the particular atmospheric layer  $i$  and the vertical column density  $VCD_i$  of this layer:

$$AMF_{iz} = \frac{SCD_{iz}}{VCD_i} \quad (1)$$

Equation (1) is strictly valid for cases of weak absorption which is the case for OCIO and  $\text{NO}_2$  in the wavelength regions considered in the study. The box AMFs depicted in Fig. 4 demonstrate only the sensitivity to vertically resolved but horizontally homogeneous atmospheric layers.

## Horizontal gradients in limb measurements of scattered sunlight

J. Pušk̄ite et al.

Title Page

Abstract

Introduction

Conclusions

References

Tables

Figures

⏪

⏩

◀

▶

Back

Close

Full Screen / Esc

Printer-friendly Version

Interactive Discussion

For the 2-D inversion the air mass factors are defined as varying not only in altitude but also in latitude  $j$ :

$$AMF_{ijz} = \frac{SCD_{ijz}}{VCD_{ij}} \quad (2)$$

The 2-D box AMFs describe the spatial character of the sensitivity of limb measurements in a more appropriate way, see Fig. 5. The enhanced sensitivity for regions crossed by the line of sight can be nicely seen; also the higher sensitivity for the instrument side can be realized. The spatial distribution of 2-D box AMFs for different elevations of the instrument's LOS is depicted in Fig. 6 for a pure Rayleigh atmosphere i.e. without clouds and aerosols. The latitudinal borders of the boxes are selected as midpoints between the tangent points (TP) of the scanning sequences of the instrument. Because of increased Rayleigh scattering at low elevation of LOS (see example given for elevation of 9 km in the Fig. 6) the contribution of light to the measurement is small close to TP (TP for the given example is at 61.8° N) and therefore the sensitivity for low altitudes (<15 km) around the TP is low. The sensitivity increases with elevation altitude. Since the box AMFs are dependent on the slantness of the light paths, large values and thus high sensitivity for high elevations occur around the TP. The fact that the light after the last scattering event moves towards the instrument along a very slant trajectory leads to high values of 2-D box AMFs along the line of sight.

Figure 6 illustrates also the wavelength dependency of the box AMFs: Due to larger probability of Rayleigh scattering for smaller wavelengths the box AMFs at 380 nm are decreased with respect to the box AMFs at 435 nm.

## 5 Results

As an example we show retrievals of NO<sub>2</sub> and OCIO number density profiles for selected orbits in January 2005. The retrieval is performed applying either 1-D or 2-D

### Horizontal gradients in limb measurements of scattered sunlight

J. Puķīte et al.

Title Page

Abstract

Introduction

Conclusions

References

Tables

Figures

◀

▶

◀

▶

Back

Close

Full Screen / Esc

Printer-friendly Version

Interactive Discussion

box AMFs in order to investigate if the 2-D box AMF concept can improve the profile retrieval for situations where the distribution of the considered trace gas along the LOS is inhomogeneous. The left panel in Fig. 7 shows the geolocation of the tangent points corresponding to the limb measurement sequences of orbit 15 122 on 20 January 2005. The right panel gives an illustration of the potential vorticity at the 475 K level (approx. 19 km altitude) above the North Pole for the same day. The position of the considered SCIAMACHY observations in the northern part of the selected orbit is indicated with a red square in both maps (approx. 55° to 70° N).

The interesting limb scanning sequences are located at the boundary of the polar vortex. Thus, due to denoxification inside the polar vortex, a strong negative gradient along the LOS (from the TP towards instrument) is expected for NO<sub>2</sub>. Vice versa, for OCIO a positive gradient is expected due to strong chlorine activation inside the polar vortex in the extraordinary cold January 2005 (regarding stratospheric temperatures). The retrieved NO<sub>2</sub> and OCIO number densities for the northern part of the selected orbit are plotted as function of latitude and altitude, both for 1-D and 2-D approach, in Figs. 8 and 9 (left and right panels, respectively). It can be seen very clearly that the NO<sub>2</sub> number density is decreasing monotonically from 60° to 70° N (in particular at the peak altitude of approx. 28 km). For OCIO, a rapid increase occurs from 65° to 70° N for altitudes between 15 and 18 km. Comparing the retrieved profiles for the 1-D and 2-D approach (dashed lines in Fig. 8 and lower panel in Fig. 9), significant differences appear. For the NO<sub>2</sub> retrieval (left panels of Figs. 8 and 9) an increase of the values in the 2-D approach is visible for altitudes from 21 to 30 km and latitude regions of 61–64° and 64–67° (dashed red and green lines respectively). While the largest increase from 0.8 to 1.2 × 10<sup>9</sup> i.e. 50% occurs at 27 km altitude for latitudes of 61–64° N, the typical difference is around 20%.

As can be seen from Fig. 6, the LOS for the 3rd scanning sequence (TP located at ~63.5° N) crosses also regions of 64–67° N for a wide altitude range (~20 km). In the 1-D retrieval, where a homogeneous distribution is assumed, the SCD retrieved in the first step of the retrieval (see Sect. 2) is accounted only as a superposition of the trace

---

## Horizontal gradients in limb measurements of scattered sunlight

J. Puškūte et al.

---

[Title Page](#)[Abstract](#)[Introduction](#)[Conclusions](#)[References](#)[Tables](#)[Figures](#)[⏪](#)[⏩](#)[◀](#)[▶](#)[Back](#)[Close](#)[Full Screen / Esc](#)[Printer-friendly Version](#)[Interactive Discussion](#)

gas abundances at different altitude levels. Therefore, also horizontal gradients will be (wrongly) accounted as vertical number density changes. In other words, a decreased measurement value due to lower NO<sub>2</sub> values towards instrument will be interpreted as a decrease in concentration values retrieved. However in the 2-D retrieval approach, the model uses knowledge from the previous state assigning part of the measured SCDs to lower concentrations more to the North. For the same example of consecutive limb scanning sequences in the northern part of the orbit 15 122 we applied the 2-D approach on the retrieval of OCIO profiles (see right panels in the Figs. 8 and 9).

Although the relative retrieval errors for OCIO are larger (in comparison with NO<sub>2</sub> retrieval), systematically lower concentrations for 2-D retrieval of OCIO can be seen for latitudes below 67° N (or for regions 64–67° N (green line) and 61–64° N (red line) corresponding to the second and third scanning sequence). Hence the 2-D approach results in a more rapid decrease of OCIO when leaving polar vortex, which is in better agreement with expectations. For the example of orbit 15 122 demonstrated in the Figs. 8 and 9 the strongest gradient of NO<sub>2</sub> occurs when crossing the border of the Arctic polar vortex (as depicted in Fig. 7, right panel). Also the rapid decrease of OCIO is observed here. Other examples where strong gradients of NO<sub>2</sub> occur are depicted in Fig. 10 for orbits 14 979 on 10 January 2005 (panel a), 15 080 on 17 January 2005 (panel b), 15 088 on 18 January 2005 (panel c) and 15 149 on 22 January 2005 (panel d).

The largest improvements occur if the gradient is strong and appears for an extended altitude interval, see e.g. results for orbit 14 979 (latitude regions corresponding to scanning sequences 3 and 4), results for orbits 15 080 and 15 149 (latitude regions corresponding to scanning sequences 2 and 3 and also 3 and 4), and results for orbit 15 088 (scanning sequences 2 and 3), shown in Fig. 10. It can be seen that the disagreement between the 1-D and 2-D retrievals increases for lower altitudes if a strong gradient exists. Also for OCIO large difference between 1-D and 2-D retrievals can be found as illustrated in Fig. 11. For many cases a decrease in the OCIO concentrations of 50% and more is found.

## Horizontal gradients in limb measurements of scattered sunlight

J. Puškūte et al.

Title Page

Abstract

Introduction

Conclusions

References

Tables

Figures

◀

▶

◀

▶

Back

Close

Full Screen / Esc

Printer-friendly Version

Interactive Discussion

In order to verify that the difference in the retrieval results for the 2-D approach is indeed resulting from an improved description of the measurement sensitivity regions, we also selected a case (orbit 15 146 on 22 January 2005) when practically no gradient for NO<sub>2</sub> is observed for the most northern part of orbit, see Fig. 12. Here the retrieval applying either 1-D or 2-D box AMFs is resulting in very similar profiles. Thus, by utilizing the overlap of consecutive limb scanning sequences, the 2-D approach allows an improved inversion of the related measurements. It has been demonstrated that this approach is correcting for the effect of horizontal gradients in limb retrievals. Such gradients can occur for several stratospheric trace gases due to their dependence on meteorological conditions, transport, solar illumination and photochemistry.

For the first limb scanning sequence of an orbit, where there is no overlap with preceding measurements, strong gradients in photochemical active species like NO<sub>2</sub> or OCIO can occur, especially for large SZA. A method to correct for this diurnal effect has been described by (McLinden et al., 2006). Currently, we are working on algorithm to combine this photochemical modeling with the 2-D approach presented in the article at hand.

## 6 Conclusions

SCIAMACHY provides scattered light measurements in limb geometry from which atmospheric trace gas profiles can be successfully retrieved. The two step approach (DOAS, RTM combined by optimal estimation) allows to investigate the effects of spectroscopy and radiative transfer on profiles separately. The assumption of horizontal homogeneous trace gas distributions can lead to errors in the retrieved profiles in particular at locations where strong horizontal gradients occur e.g. at the edge of polar vortex. The combination of several SCIAMACHY limb scanning sequences simultaneously in one inversion constraint allows taking into account the spatial correlation between these measurements and thereby improving the profile retrieval. The application of a simultaneous inversion of consecutive limb scanning sequences for SCIAMACHY

### Horizontal gradients in limb measurements of scattered sunlight

J. Puškūte et al.

Title Page

Abstract

Introduction

Conclusions

References

Tables

Figures

⏪

⏩

◀

▶

Back

Close

Full Screen / Esc

Printer-friendly Version

Interactive Discussion

UV/vis measurements is demonstrated for the first time. It allows the correction for cases with large horizontal gradients: concentrations and profile shape are corrected in the true direction for both types of gradients (positive and negative). By combination of this 2-D approach and photochemical modelling, a more detailed correction for horizontal gradients will be achieved in a future modification of the retrieval algorithm.

For situation with practically no horizontal gradients no difference between the 1-D and the 2-D retrieval is observed. A small distance between limb scanning sequences improves the horizontal resolution of the measurements; therefore an instrument using only UV/vis limb measurements i.e. without performing nadir observations in between two limb scanning sequences would be an advantage and further improve the accuracy of the retrieved profiles.

*Acknowledgements.* We want to thank ESA for providing data of SCIAMACHY, DLR for providing the SCIAMACHY geolocation maps via SOST webpage (<http://atmos.caf.dlr.de/projects/scops/>), NILU and ECMWF for meteorological data, University of Latvia and ESF for support. One author (S. Köhl) is funded by the DFG (Deutsche Forschungs Gemeinschaft).

## References

- Bovensmann H., Burrows, J. P., Buchwitz, M., Frerick, J., Noël, S., Rozanov, V. V., Chance, K. V., and Goede, A. P. H.: SCIAMACHY: Mission objectives and measurement modes, *J. Atmos. Sci.*, 56, 127–150, 1999. [16157](#)
- Brühl, C. and Crutzen, P. J.: MPIC two-dimensional model, in: *The Atmospheric Effect of Stratospheric Aircraft*, 1292, edited by: Prather, M. J. and Remsberg, E. E., NASA Ref. Publications, pp. 103–104, 1993. [16160](#)
- Butz A., Boesch, H., Camy-Peyret, C., Chipperfield, M., Dorf, M., Dufour, G., Grunow, K., Jeseck, P., Köhl, S., Payan, S., Pepin, I., Puķīte, J., Rozanov, A., von Savigny, C., Sioris, C., Wagner, T., Weidner, F., and Pfeilsticker, K.: Inter-comparison of stratospheric O<sub>3</sub> and NO<sub>2</sub> abundances retrieved from balloon borne direct sun observations and Envisat/SCIAMACHY limb measurements, *Atmos. Chem. Phys.*, 6, 1293–1314, 2006, <http://www.atmos-chem-phys.net/6/1293/2006/>. [16159](#)
- Carlotti, M., Brizzi, G., Papandrea, E., Prevedelli, M., Ridolfi, M., Dinelli, B. M., and Magnani, L.:

## Horizontal gradients in limb measurements of scattered sunlight

J. Puķīte et al.

Title Page

Abstract

Introduction

Conclusions

References

Tables

Figures

◀

▶

◀

▶

Back

Close

Full Screen / Esc

Printer-friendly Version

Interactive Discussion

---

**Horizontal gradients  
in limb  
measurements of  
scattered sunlight**

---

J. Puķīte et al.

Title Page

Abstract

Introduction

Conclusions

References

Tables

Figures

◀

▶

◀

▶

Back

Close

Full Screen / Esc

Printer-friendly Version

Interactive Discussion

GMTR: Two-dimensional geo-fit multitarget retrieval model for Michelson Interferometer for Passive Atmospheric Sounding/Environmental Satellite observations, Appl. Opt., 45, 716–727, 2006. [16158](#)

5 Carlotti, M., Dinelli, B. M., Raspollini, P., and Ridolfi, M.: Geo-fit Approach to the Analysis of Limb-Scanning Satellite Measurements, Appl. Opt. 40, 1872–1885, 2001. [16158](#)

Deutschmann, T. and Wagner, T.: TRACY-II Users manual, University of Heidelberg, Heidelberg, Germany, 2007. [16159](#)

10 Dorf M., Boesch, H., Butz, A., Camy-Peyret, C., Chipperfield, M. P., Engel, A., Goutail, F., Grunow, K., Hendrick, F., Hrechanyy, S., Naujokat, B., Pommereau, J.-P., Van Roozendael, M., Sioris, C., Stroh, F., Weidner, F., and Pfeilsticker, K.: Balloon-borne stratospheric BrO measurements: Comparison with Envisat/SCIAMACHY BrO limb profiles, Atmos. Chem. Phys., 6, 2483–2501, 2006, <http://www.atmos-chem-phys.net/6/2483/2006/>. [16159](#)

European Centre for Medium-Range Weather Forecasts (ECMWF): Temperature and potential vorticity analyses, Dan. Meteorol. Inst., Copenhagen, 2000. [16178](#)

15 Haley, C. S., Brohede, S. M., Sioris, C. E., Griffioen, E., Murtagh, D. P., McDade, I. C., Eriksson, P., Llewellyn, E. J., Bazureau, A., and Goutail, F.: Retrieval of stratospheric O<sub>3</sub> and NO<sub>3</sub> profiles from Odin Optical Spectrograph and Infrared Imager System (OSIRIS) limb-scattered sunlight measurements, J. Geophys. Res., 109, D16303, doi:10.1029/2004JD004588, 2004. [16158](#)

20 Krecl, P., Haley, C. S., Stegman, J., Brohede, S. M., and Berthet G.: Retrieving the vertical distribution of stratospheric OCIO from Odin/OSIRIS limb-scattered sunlight measurements, Atmos. Chem. Phys., 6, 1879–1894, 2006, <http://www.atmos-chem-phys.net/6/1879/2006/>. [16158](#)

25 K hl, S.: Quantifying Stratospheric chlorine chemistry by the satellite spectrometers GOME and SCIAMACHY, PhD Thesis, Universit t Heidelberg, Heidelberg, Germany, 177 pp., available at: <http://www.ub.uni-heidelberg.de/archiv/5664/>, 2005. [16157](#), [16158](#), [16159](#)

K hl, S., Puķ ite, J., Deutschmann, T., Platt, U., and Wagner, T.: SCIAMACHY Limb Measurements of NO<sub>2</sub>, BrO and OCIO, Retrieval of vertical profiles: Algorithm, first results and validation, in press, doi:10.1016/j.asr.2007.10.022, Adv. Space Res., 2007. [16157](#), [16158](#), [16159](#)

30 Llewellyn E. J., Lloyd, N. D., Degenstein, D. A., Gattinger, R. L., Petelina, S. V., Bourassa, A. E., Wiensz, J. T., Ivanov, E. V., McDade, I. C., Solheim, B. H., McConnell, J. C., Haley, C. S., von Savigny, C., Sioris, C. E., McLinden, C. A., Griffioen, E., Kaminski, J., Evans,

---

**Horizontal gradients  
in limb  
measurements of  
scattered sunlight**

---

J. Puķīte et al.

Title Page

Abstract

Introduction

Conclusions

References

Tables

Figures

◀

▶

◀

▶

Back

Close

Full Screen / Esc

Printer-friendly Version

Interactive Discussion

W. F. J., Puckrin, E., Strong, K., Wehrle, V., Hum, R. H., Kendall, D. J. W., Matsushita, J., Murtagh, D. P., Brohede, S., Stegman, J., Witt, G., Barnes, G., Payne, W. F., Piché, L., Smith, K., Warshaw, G., Deslauniers, D.-L., Marchand, P., Richardson, E. H., King, R. A., Wevers, I., McCreath, W., Kyrölä, E., Oikarinen, L., Leppelmeier, G. W., Auvinen, H., Mégie, G., Hauchecorne, A., Lefèvre, F., de La Nöe, J., Ricaud, P., Frisk, U., Sjöberg, F., von Schéele, F., and Nordh, L.: The OSIRIS instrument on the Odin spacecraft, *Can. J. Phys.*, 82, 411–422, 2004. [16157](#)

Loughman, R. P., Griffioen, E., Oikarinen, L., Postlyakov, O. V., Rozanov, A., Flittner, D. E., and Rault, D. F.: Comparison of radiative transfer models for limb-viewing scattered sunlight measurements, *J. Geophys. Res.*, 109, D06303, doi:10.1029/2003JD003854, 2004. [16159](#)

McLinden, C. A., Haley, C. S., and Sioris, C. E.: Diurnal effects in limb scatter observations, *J. Geophys. Res.*, 111, D14302, doi:10.1029/2005JD006628, 2006. [16158](#), [16166](#)

Natarajan, M., Deaver, L. E., Thompson, E., and Magill, B.: Impact of twilight gradients on the retrieval of mesospheric ozone from HALOE, *J. Geophys. Res.*, 110, D13305, doi:10.1029/2004JD005719, 2005. [16158](#)

Oikarinen, L., Sihvola, E., and Kyrölä, E.: Multiple-scattering radiance in limb-viewing geometry, *J. Geophys. Res.*, 104, 31 261–31 274, 1999. [16159](#)

Puķīte, J., Kühn, S., Deutschmann, T., Wilms-Grabe, W., Friedeburg, C., Platt, U., and Wagner, T.: Retrieval of stratospheric trace gases from SCIAMACHY limb measurements, Proceedings of the First Atmospheric Science Conference, 8–12 May, ESA/ESRIN, Frascati, Italy, ESA SP-628, available at: [http://earth.esa.int/workshops/atmos2006/participants/1148/paper\\_proc\\_Frasc.2.pdf](http://earth.esa.int/workshops/atmos2006/participants/1148/paper_proc_Frasc.2.pdf), 2006. [16157](#), [16158](#), [16159](#)

Rault D. F.: Ozone profile retrieval from Stratospheric Aerosol and Gas Experiment (SAGE III) limb scatter measurements, *J. Geophys. Res.*, 110, D09309, doi:10.1029/2004JD004970, 2005. [16157](#)

Ridolfi, M., Magnani, L., Carlotti, M., and Dinelli, B. M.: MIPAS-ENVISAT Limb-Sounding Measurements: Trade-Off Study for Improvement of Horizontal Resolution, *Appl. Opt.*, 43, 5814–5824, 2004. [16158](#)

Rozanov, A., Bovensmann, H., Bracher, A., Hrechanyy, S., Rozanov, V., Sinnhuber, M., Stroth, F., and Burrows, J. P.: NO<sub>2</sub> and BrO vertical profile retrieval from SCIAMACHY limb measurements: sensitivity studies, *Adv. Space Res.*, 36, 846–854., 2005. [16157](#)

Sinnhuber, B.-M., Rozanov, A., Sheode, N., Afe, O. T., Richter, A., Sinnhuber, M., Wittrock, F., and Burrows, J. P.: Global observations of stratospheric bromine monoxide from SCIA-

MACHY, Geophys. Res. Lett., 32, L20810, 2005. [16157](#)

Sioris, C. E., Kovalenko, L. J., McLinden, C. A., Salawitch, R. J., Van Roozendael, M., Goutail, F., Dorf, M. Pfeilsticker, K., Chance, K., von Savigny, C., Liu, X., Kurosu, T. P., Pomereau, J.-P., Bosch, H., and Frerick, J.: Latitudinal and vertical distribution of bromine monoxide in the lower stratosphere from Scanning Imaging Absorption Spectrometer for Atmospheric Chartography limb scattering measurements, J. Geophys. Res., 111, D14301, doi:10.1029/2005JD006479, 2006. [16157](#), [16158](#), [16159](#)

Sioris, C. E., Kurosu, T. P., Martin, R. V., and Chance, K.: Stratospheric and tropospheric NO<sub>2</sub> observed by SCIAMACHY: First results, Adv. Space Res., 34, 780–785, 2004. [16157](#)

Wagner, T., Burrows, J. P., Deutschmann, T., Dix, B., von Friedeburg, C., Frieß, U., Hendrick, F., Heue, K.-P., Irie, H., Iwabuchi, H., Kanaya, Y., Keller, J., McLinden, C. A., Oetjen, H., Palazzi, E., Petritoli, A., Platt, U., Postlyakov, O., Puķīte, J., Richter, A., van Roozendael, M., Rozanov, A., Rozanov, V., Sinreich, R., Sanghavi, S., and Wittrock, F.: Comparison of Box-Air-Mass-Factors and Radiances for Multiple-Axis Differential Optical Absorption Spectroscopy (MAX-DOAS) Geometries calculated from different UV/visible Radiative Transfer Models, Atmos. Chem. Phys., 7, 1809–1833, 2007,

<http://www.atmos-chem-phys.net/7/1809/2007/>. [16159](#)

ACPD

7, 16155–16183, 2007

---

## Horizontal gradients in limb measurements of scattered sunlight

J. Puķīte et al.

---

Title Page

Abstract

Introduction

Conclusions

References

Tables

Figures

◀

▶

◀

▶

Back

Close

Full Screen / Esc

Printer-friendly Version

Interactive Discussion

**Horizontal gradients  
in limb  
measurements of  
scattered sunlight**

J. Puķīte et al.

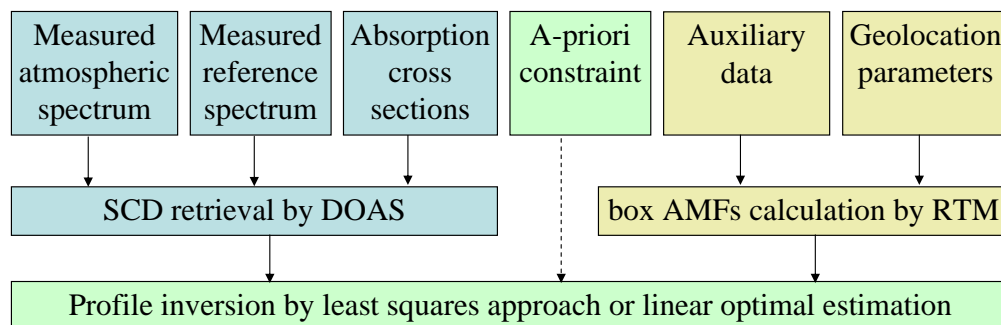


**Fig. 1.** Schematic diagram of the algorithm applied for profile retrieval.

[Title Page](#)[Abstract](#)[Introduction](#)[Conclusions](#)[References](#)[Tables](#)[Figures](#)[◀](#)[▶](#)[◀](#)[▶](#)[Back](#)[Close](#)[Full Screen / Esc](#)[Printer-friendly Version](#)[Interactive Discussion](#)

## Horizontal gradients in limb measurements of scattered sunlight

J. Puķīte et al.

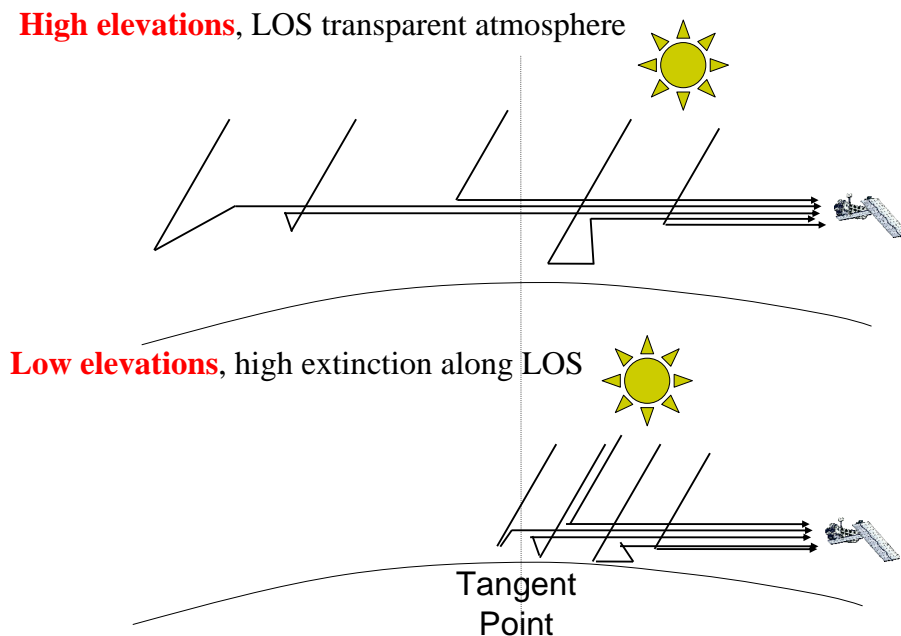


**Fig. 2.** Schematic view of the spatial sensitivity distribution. Contributing light paths are displayed. More crossing paths means higher sensitivity for a particular region.

Title Page

Abstract

Introduction

Conclusions

References

Tables

Figures

◀

▶

◀

▶

Back

Close

Full Screen / Esc

Printer-friendly Version

Interactive Discussion

**Horizontal gradients  
in limb  
measurements of  
scattered sunlight**

J. Puķīte et al.

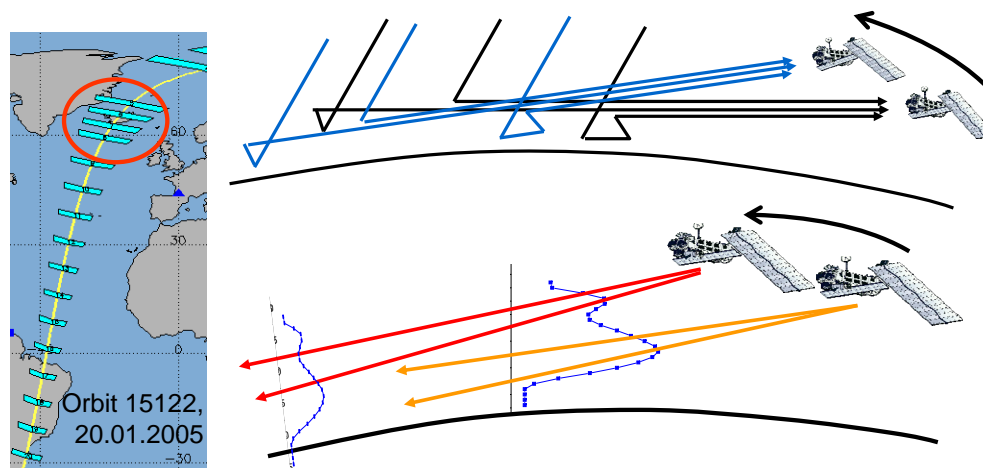


**Fig. 3.** Spatial correlation of two successive limb scanning sequences (right panel) together with a geolocation map of the SCIAMACHY limb scanning sequences (left panel, taken from SOST webpage: [atmos.caf.dlr.de/projects/scops/](http://atmos.caf.dlr.de/projects/scops/)). If the distance is small enough for the measurement regions to partially overlap, as for scanning sequences indicated with red circle (left panel), the measurement of the same air masses is made from different instrument positions.

Title Page

Abstract

Introduction

Conclusions

References

Tables

Figures

◀

▶

◀

▶

Back

Close

Full Screen / Esc

Printer-friendly Version

Interactive Discussion

## Horizontal gradients in limb measurements of scattered sunlight

J. Puķīte et al.

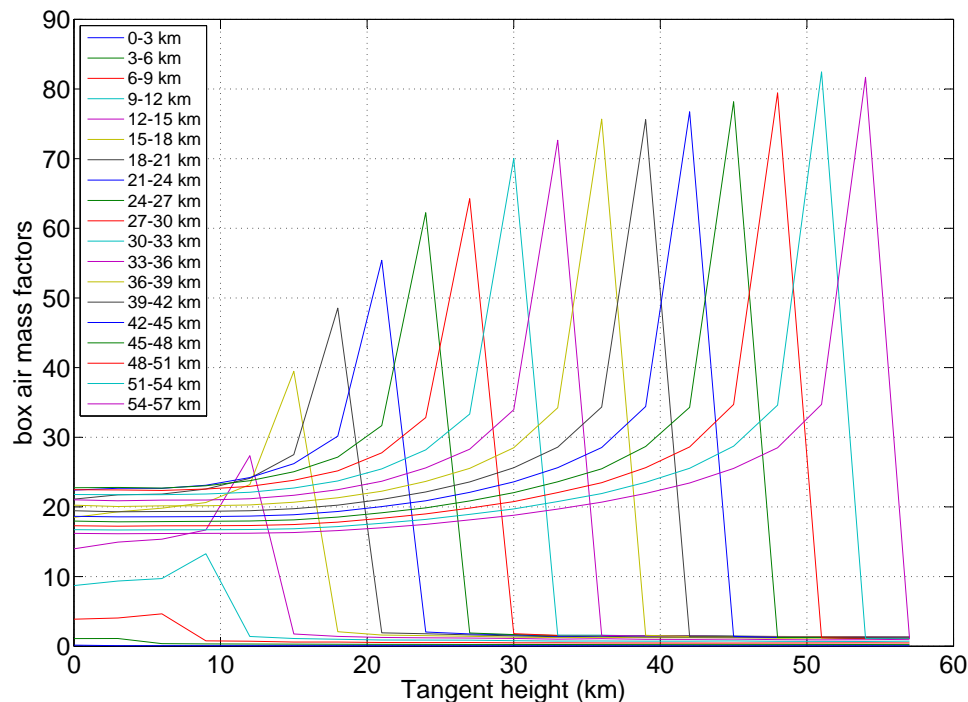


**Fig. 4.** One dimensional box AMFs for 435 nm plotted for 3 km thick boxes as function of the tangent height. Illustration are for the 3rd scanning sequence (solar zenith angle:  $84^\circ$ ; solar azimuth angle:  $-44^\circ$  at the tangent point) in the descending part from North of an orbit of SCIAMACHY in the middle of January (orbit 15 149 on 22 January 2005). The peak value usually is located at the tangent height equal to the altitude of the “box” simulated.

Title Page

Abstract

Introduction

Conclusions

References

Tables

Figures

◀

▶

◀

▶

Back

Close

Full Screen / Esc

Printer-friendly Version

Interactive Discussion

## Horizontal gradients in limb measurements of scattered sunlight

J. Puķīte et al.

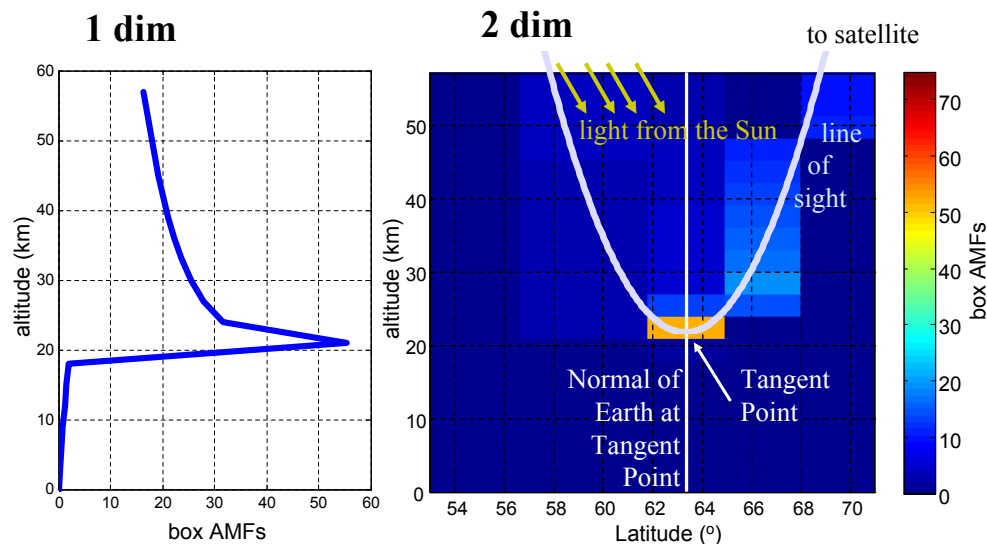


**Fig. 5.** Comparison between 1-D and 2-D box air mass factors. Values calculated for 435 nm are plotted for an elevation with tangent height at 21 km. Illustrations are for the 3rd scanning sequence (solar zenith angle:  $84^\circ$ ; solar azimuth angle:  $-44^\circ$  at the tangent point) in the descending part from North of an orbit of SCIAMACHY in the middle of January (orbit 15 149 on 22 January 2005). The latitudinal distribution of the air mass factor along the line of sight of the instrument can be realized for 2-D box AMFs. Introducing 2-D AMFs in the retrieval is discretizing air masses measured not only in altitude but also in latitude.  $1^\circ$  of latitude corresponds to  $\sim 119$ – $160$  km depending on line of sight azimuth angle. Line of sight, normal of the Earth, tangent point, and direction of Sun light are also shown in the figure.

Title Page

Abstract

Introduction

Conclusions

References

Tables

Figures

◀

▶

◀

▶

Back

Close

Full Screen / Esc

Printer-friendly Version

Interactive Discussion

## Horizontal gradients in limb measurements of scattered sunlight

J. Puškūte et al.

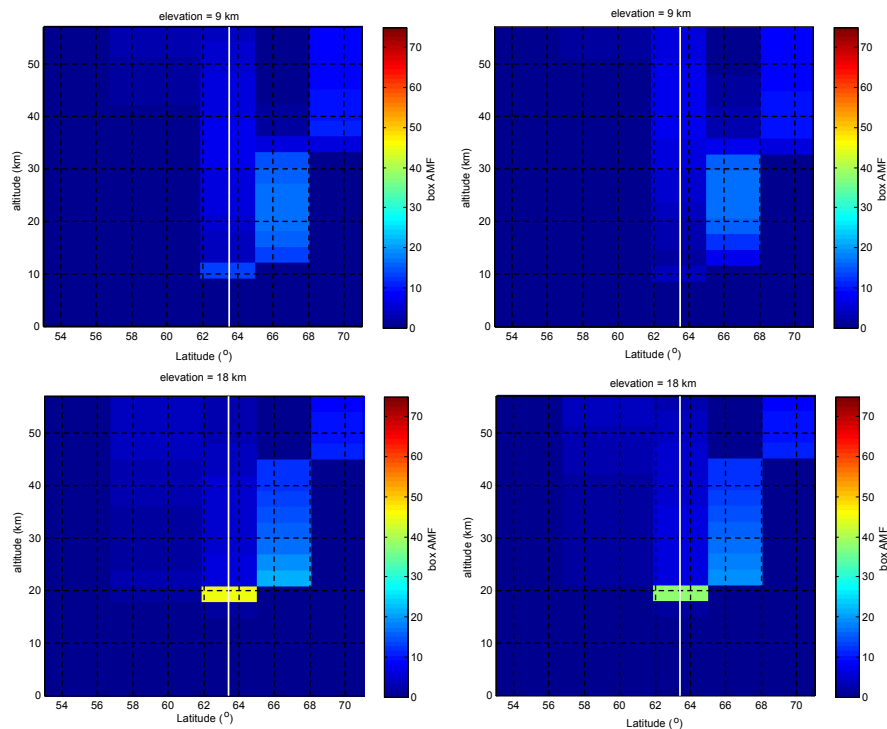


**Fig. 6.** 2-D AMFs for different elevations as modelled by the RTM model Tracy-II for 435 nm ( $\text{NO}_2$ ) on the left panel and 380 nm (OCIO) on the right panel. Values are plotted for the example of the 3rd scanning sequence in the descending part from North of an orbit of SCIAMACHY in the middle of January (orbit 15 149 on 22 January 2005). Normal from tangent point to the Earth surface is indicated with a white line.

[Title Page](#)[Abstract](#)[Introduction](#)[Conclusions](#)[References](#)[Tables](#)[Figures](#)[⏪](#)[⏩](#)[◀](#)[▶](#)[Back](#)[Close](#)[Full Screen / Esc](#)[Printer-friendly Version](#)[Interactive Discussion](#)

---

**Horizontal gradients  
in limb  
measurements of  
scattered sunlight**

---

J. Puķīte et al.

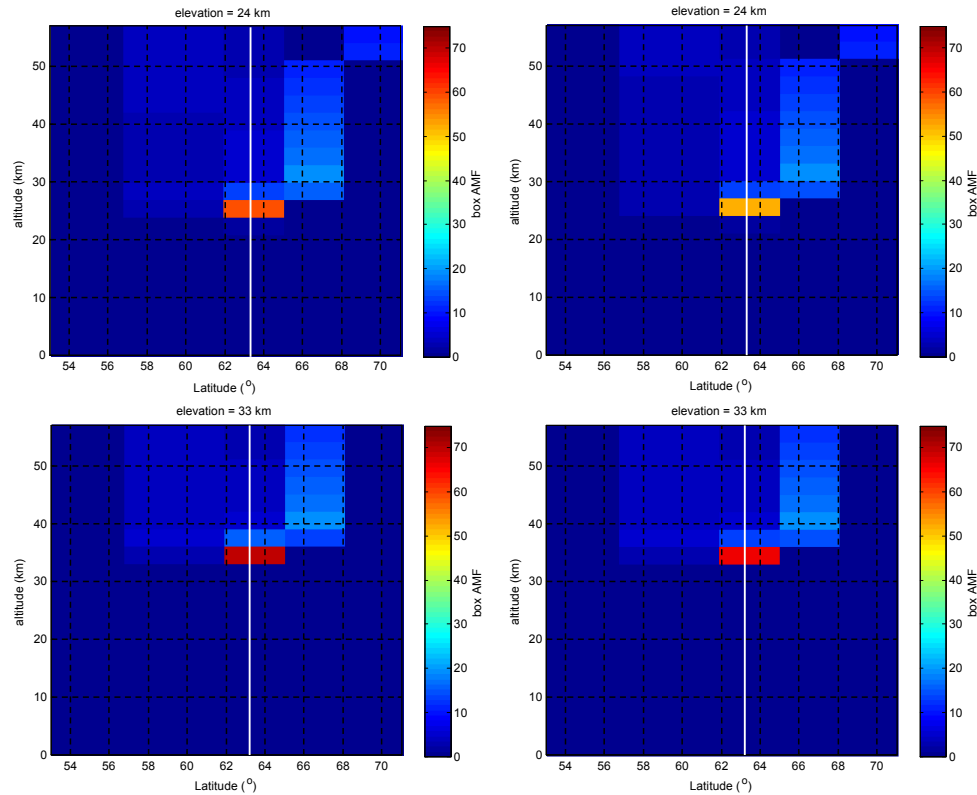
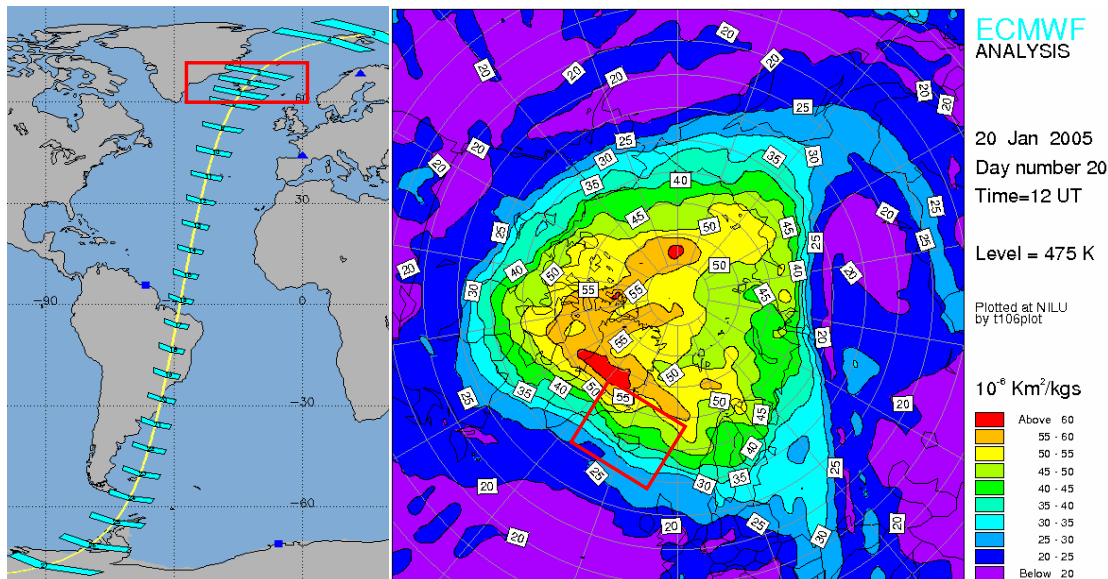
[Title Page](#)[Abstract](#)[Introduction](#)[Conclusions](#)[References](#)[Tables](#)[Figures](#)[⏪](#)[⏩](#)[◀](#)[▶](#)[Back](#)[Close](#)[Full Screen / Esc](#)[Printer-friendly Version](#)[Interactive Discussion](#)

Fig. 6. Continued.

## Horizontal gradients in limb measurements of scattered sunlight

J. Puķīte et al.



**Fig. 7.** Left panel shows geolocations of the tangent points for the limb scanning sequences of the orbit 15 122 on 20 January 2005. The red box indicates the states for which the retrieval is shown in the line plots in Fig. 8. Potential vorticity for the same day, 12:00 UT is displayed in the right panel (ECMWF, 2000).

Title Page

Abstract

Introduction

Conclusions

References

Tables

Figures

⏪

⏩

◀

▶

Back

Close

Full Screen / Esc

Printer-friendly Version

Interactive Discussion

**Horizontal gradients  
in limb  
measurements of  
scattered sunlight**

J. Puķīte et al.

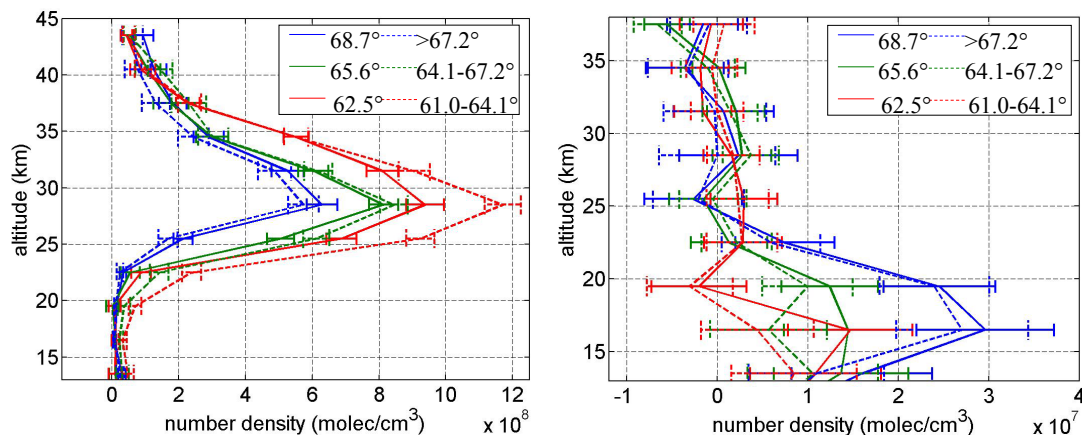


**Fig. 8.** Comparison between retrieved profiles using 1-D approach (solid lines) and 2-D approach (dashed lines) for orbit 15 122 on 20 January 2005 for NO<sub>2</sub> (left panel) and OCIO (right panel) for the first three northern states of descending part of the orbit (see also Figs. 7 and 9).

[Title Page](#)[Abstract](#)[Introduction](#)[Conclusions](#)[References](#)[Tables](#)[Figures](#)[◀](#)[▶](#)[◀](#)[▶](#)[Back](#)[Close](#)[Full Screen / Esc](#)[Printer-friendly Version](#)[Interactive Discussion](#)

## Horizontal gradients in limb measurements of scattered sunlight

J. Puķīte et al.

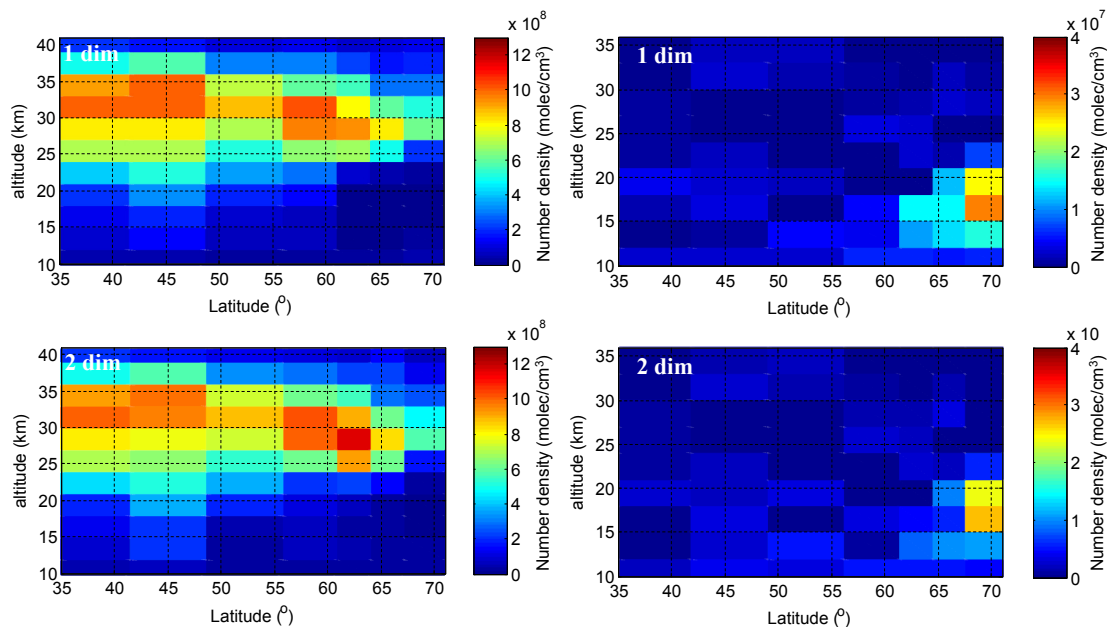


**Fig. 9.** Comparison between retrieved profiles using 1-D approach (upper panel) and 2-D approach (bottom line) for orbit 15 122 on 20 January 2005 for NO<sub>2</sub> (left panel) and OCIO (right panel) for northern part of orbit 15 122 (see also Figs. 7 and 8). An improvement for the 2-D retrieval with respect to the 1-D approach for the most northern states with higher latitudinal resolution can be seen.

[Title Page](#)[Abstract](#)[Introduction](#)[Conclusions](#)[References](#)[Tables](#)[Figures](#)[⏪](#)[⏩](#)[◀](#)[▶](#)[Back](#)[Close](#)[Full Screen / Esc](#)[Printer-friendly Version](#)[Interactive Discussion](#)

## Horizontal gradients in limb measurements of scattered sunlight

J. Puškūte et al.

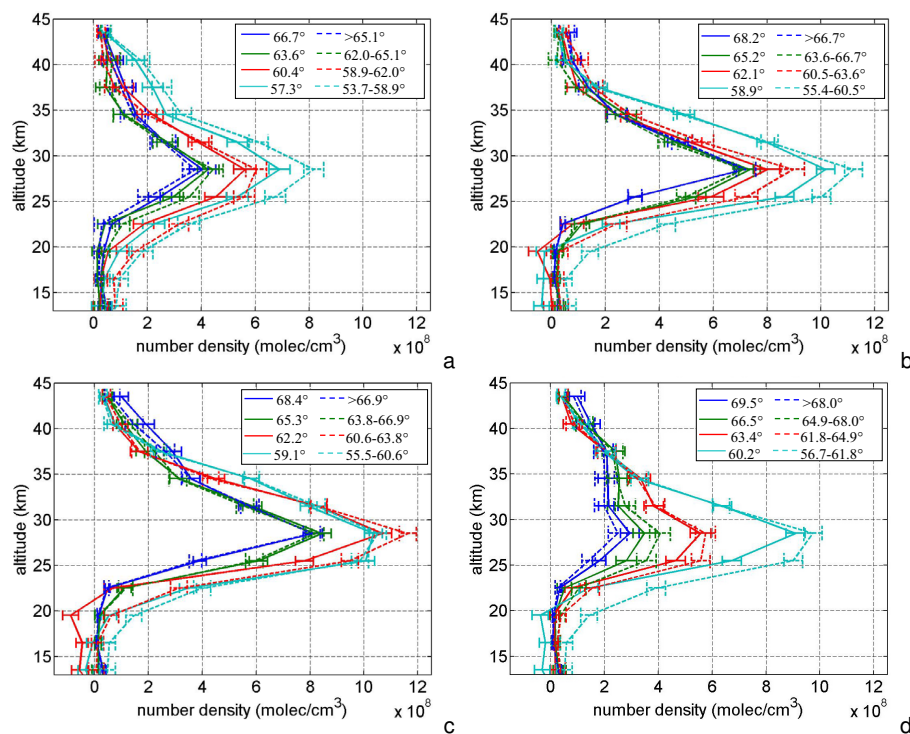


**Fig. 10.** Comparison between retrieved profiles of  $\text{NO}_2$  made separately for every scanning sequence i.e. applying 1-D box air mass factors (solid lines) or performing profile inversions for all scanning sequences at the same time i.e. applying 2-D box air mass factors (dashed lines). Results for the first 4 latitudinal regions (2-D retrieval) or scanning sequences (1-D retrieval) are displayed as they follow from the North in blue, green, red and cyan. The results are displayed for orbits 14 979 on 10 January 2005 (panel a), 15 080 on 17 January 2005 (panel b), 15 088 on 18 January 2005 (panel c) and 15 149 on 22 January 2005 (panel d).

Title Page

Abstract

Introduction

Conclusions

References

Tables

Figures

◀

▶

◀

▶

Back

Close

Full Screen / Esc

Printer-friendly Version

Interactive Discussion

## Horizontal gradients in limb measurements of scattered sunlight

J. Puškūte et al.

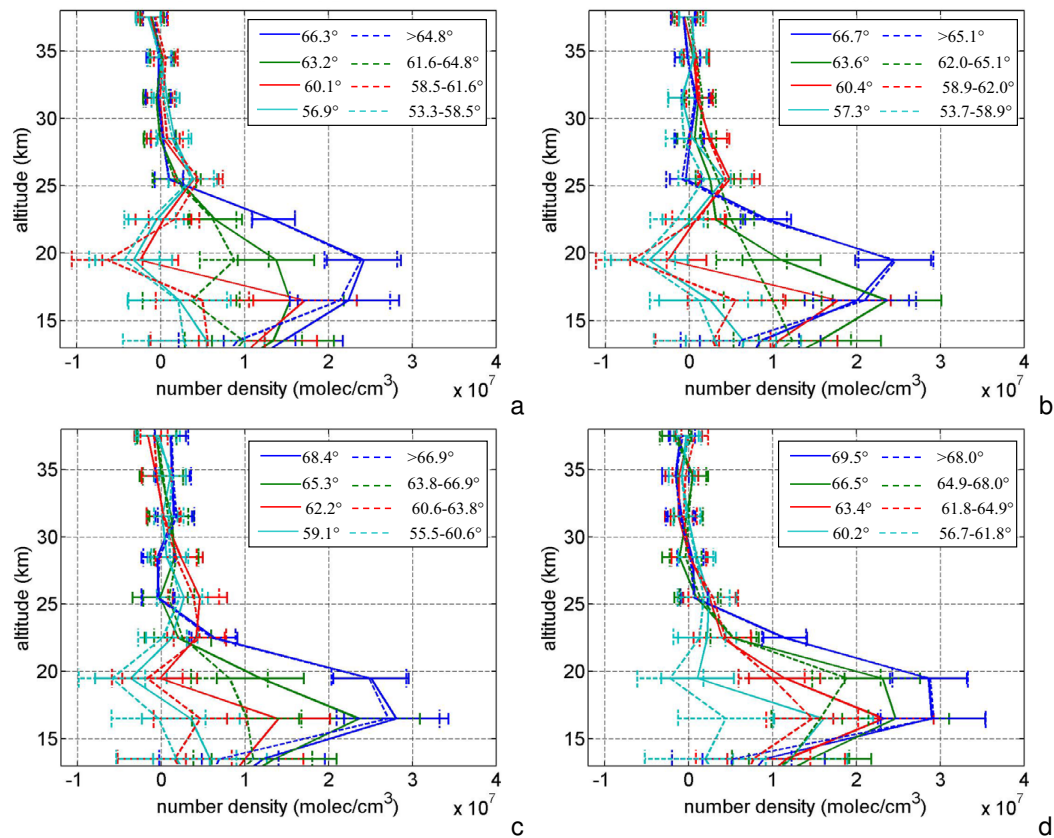


**Fig. 11.** The same as in Fig. 10 but for OCIO for orbits 14951 on 8 January 2005 (panel a), 14979 on 10 January 2005 (panel b), 15088 on 18 January 2005 (panel c) and 15149 on 22 January 2005 (panel d).

[Title Page](#)
[Abstract](#)
[Introduction](#)
[Conclusions](#)
[References](#)
[Tables](#)
[Figures](#)
[◀](#)
[▶](#)
[◀](#)
[▶](#)
[Back](#)
[Close](#)
[Full Screen / Esc](#)
[Printer-friendly Version](#)
[Interactive Discussion](#)

**Horizontal gradients  
in limb  
measurements of  
scattered sunlight**

J. Puķīte et al.

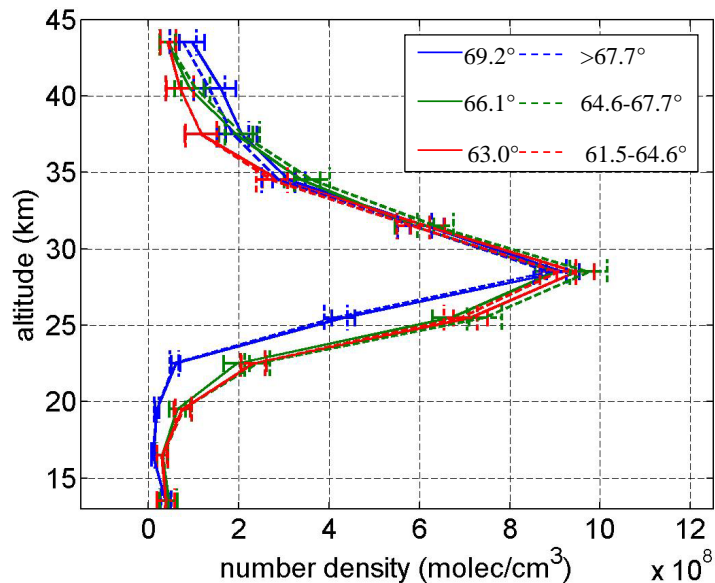


**Fig. 12.** Comparison between retrieved profiles using 1-D approach (solid lines) and 2-D approach (dashed lines) for orbit 15 146 on 22 January 2005 for NO<sub>2</sub> for the first three northern states of descending part of the orbit.

[Title Page](#)[Abstract](#)[Introduction](#)[Conclusions](#)[References](#)[Tables](#)[Figures](#)[◀](#)[▶](#)[◀](#)[▶](#)[Back](#)[Close](#)[Full Screen / Esc](#)[Printer-friendly Version](#)[Interactive Discussion](#)